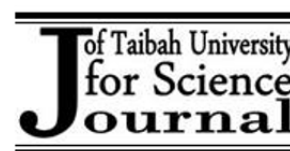




Available online at www.taibahu.edu.sa
ISSN: 1658-3655
Alamri et.al. / JTUSCI 1: 35-43 (2008)



Structural and optical properties of 1, 4, 8, 11, 15, 18, 22, 25-octahexylphthalocyanine: A comparison between thermally evaporated and spin-coated thin films

Saleh N. Alamri^a, Ahmad A. Joraid^{a*}, Ahmed S. Solieman^a, Shaya.Y. Al-Raqa^b, Ahmed A. Mohamed^b

^aPhysics Department, Taibah University, Madinah, Saudi Arabia, ^b Chemistry Department, Taibah University, Madinah, Kingdom of Saudi Arabia

Abstract

Thin films of 1, 4, 8, 11, 15, 18, 22, 25-octahexylphthalocyanine were deposited on glass substrates by the thermal evaporation and spin coating techniques. The structure of the both types of films was found to be in α form. The crystallite size assumed the values of 88.65 and 44.32 nm for thermal and spin coated films, respectively. The surface morphology of the thin films was investigated by atomic force microscopy and showed that the molecules of 1, 4, 8, 11, 15, 18, 22, 25-octahexylphthalocyanine grew in stacks of parallel rows. The optical properties of thermally evaporated and spin coated films are reported here. The spectrophotometric measurements of transmittance and reflectance were carried out at UV-Vis-NIR region for the films that showed two absorption bands, namely the Q- and Soret bands. The mechanism of the optical absorption follows the indirect transitions. Almost there was no remarkable difference was observed between the two types of films. Other optical parameters, such as absorption coefficient α , the absorption index, k , and refractive index, n , were also determined.

Keywords: AFM, thermal evaporation, spin coating; optical properties, phthalocyanine

Introduction

Phthalocyanines have many important commercial applications such as colorants for fabrics, printing inks, ball points, and color photography. They are arguably best known for their intense blue or blue-green colours, their thermal and chemical stability, and their ability to incorporate into the center of their ring system about 70 elements of the Periodic Table [1-2].

It is important for the field of molecular electronics that highly ordered, reproducible, thin films can be achieved. There has therefore been a variety of methods reported for deposition of phthalocyanines. These include vacuum deposition, organic molecular beam epitaxy [3], Langmuir-Blodgett film formation [4], self-assembled monolayer films [5], and spin-coating technology,

which are demonstrated as a useful method of preparing oriented Pc films [6-8].

Thermal evaporation technique takes several advantages such as greater reproducibility and higher uniformity. Moreover this technique, featuring the peculiarity to produce thin solid films without using any extraneous compound, allows to deposit samples characterized by a much higher purity. Spin coating is a mature technique and uses commercially available equipment and resists. The process is compatible with the IC technology and can be used at all stages of processing on all types of substrate layers. There are only two parameters that strongly influence the layer forming, i.e. the resist solution viscosity and the spinning speed. Therefore, the process optimization focuses only on these two parameters.

In the present work thin films of metal-free 1, 4, 8, 11, 15, 18, 22, 25-octahexylphthalocyanine were thermally evaporated onto original microscope slide substrates. Another group of thin films was deposited by using spin coating technique onto the same kind of substrates. Henceforth these two groups will be denoted as H₂PC-Th and H₂PC-Sp for thermal evaporation and spin coating, respectively. The structural and optical parameters were determined and are discussed here for the sake of comparison.

Experimental

Synthesis. The metal-free phthalocyanine compound used in this study was prepared directly by cyclotetramerization of 3, 6-diethylphthalonitrile in presence of lithium butoxide in butanol. The purification steps required column chromatography on silica gel using petroleum ether as an eluent to yield 77% of 1,4,8,11,15,18,22,25-octahexylphthalocyanine compound depicted in Fig. 1. The Pc compound was characterized by nuclear magnetic resonance (¹H NMR, Bruker AVANCE 400 MHz). IR spectra were recorded on Shimadzu Fourier Transform Infrared Spectrometer (FTIR-400).

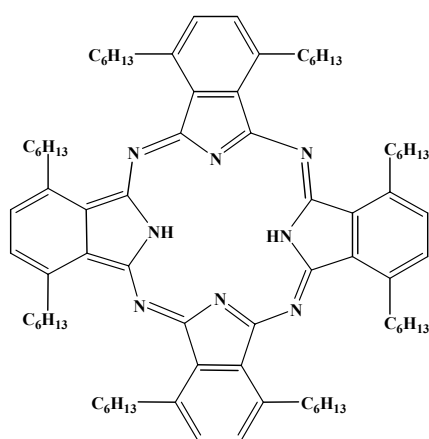


Fig. 1. The chemical structure of metal-free 1, 4, 8, 11, 15, 18, 22, 25-octahexylphthalocyanine.

The synthesized Pc complex possesses excellent solubility in various organic solvents such as

CH₂Cl₂, Tetra hydrofuran (THF), acetone and ethyl acetate, and do not readily aggregate in solution [9,10].

Instrumentation. The films were deposited onto rectangular, optically flat, standard microscope slide substrates of thickness 1 mm at room temperature. The slide substrates were carefully cleaned ultrasonically in acetone and then rinsed with deionized water. The evaporation was carried out by resistive heating of 15 mg of the material from a tungsten boat, which was heated by passing high current in a base vacuum of 7.5×10^{-8} Pa during the deposition process. The other group of films was deposited by using spin coating technique (Specialty Coating Systems G3P-8 Spin Coater) under nitrogen flow at 2000 rpm for 2 min.

The surface microstructure was demonstrated by atomic force microscopy (AFM; Veeco CP-II) in non-contact mode with Si tips at a scan rate of 1 Hz. The film thickness, deduced from AFM measurements, was estimated to be 730 nm for H₂PC-Th and in the range of 45-50 nm for H₂PC-Sp. Phthalocyanine structure was examined using a Shimadzu XRD-6000 X-ray diffractometer using *CuK α* radiation ($\lambda = 1.5418 \text{ \AA}$). The X-ray tube voltage and current were 40 kV and 30 mA respectively.

The transmittance, $T(\lambda)$, and reflectance, $R(\lambda)$, spectra of the films were measured at normal incidence and at an incident angle of 5° respectively. The measurements were obtained at room temperature in the spectral range of 300–1200 nm by using a computer-aided double-beam spectrophotometer (Shimadzu 3150 UV-VIS-NIR) with a resolution of 0.1 nm.

Results & discussion

Structural studies

The XRD diffraction patterns for H₂PC-Th and H₂PC-Sp is shown in Fig. 2.

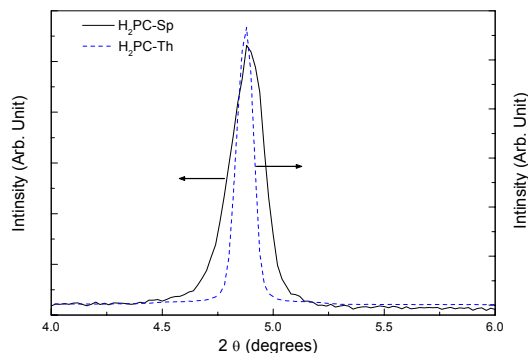


Fig. 2. X-ray diffraction pattern of metal-free thermally evaporated, H₂PC-Th and spin coated, H₂PC-Sp thin films.

It is clear from the figure that the pattern shows the α form for both samples because it does not show the characteristic double intense peak that is observed with the β form. The films show the appearance of a high-intensity peak at $2\theta = 4.88^\circ$. The individual crystallite size was determined using Scherrer's relation [9]:

$$D = \frac{S\lambda}{\beta \cos \theta}, \quad (1)$$

where S is the Scherrer constant which is equal to 0.9, λ is the wavelength of the incident radiation, β is the full width at half maximum intensity, and θ is the Bragg angle corresponding to the peak being considered. Using the values derived from the peak shown in Fig. 2, the crystallite sizes of the two samples H₂PC-Th and H₂PC-Sp was determined to be in the order of 88.65 and 44.32 nm, respectively. This increase in crystallite size may be due to pseudomorphic layers, which are formed at room temperature and in a metastable state, being destroyed by heat, which causes larger crystallites to be formed [11].

The AFM micrographs indicate that the thermal evaporated H₂PC-Th and spin coated films H₂PC-Sp were uniform, smooth and dense on glass, with a mean roughness of 1.26 and 1.49 nm, respectively. The arrangement of molecular orientations strongly depends on growth conditions and substrates. Fig. 3 (a, b) and 4 (a, b) show 2D and 3D $5 \times 5 \mu\text{m}$ AFM image of the surface of H₂PC-Th and H₂PC-Sp, respectively.

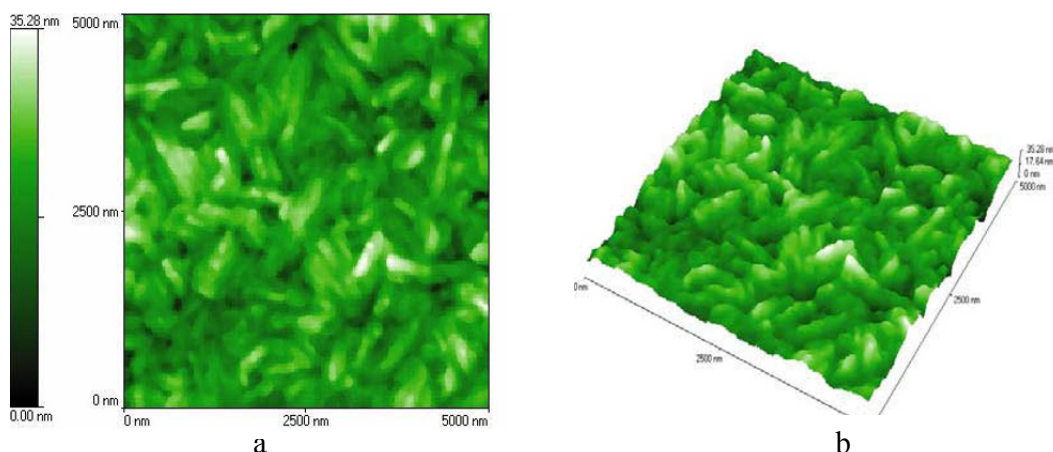


Fig. 3. $5 \mu\text{m} \times 5 \mu\text{m}$ AFM patterns of the surface of H₂PC-Th thin films: (a) 2-D and (b) 3-D.

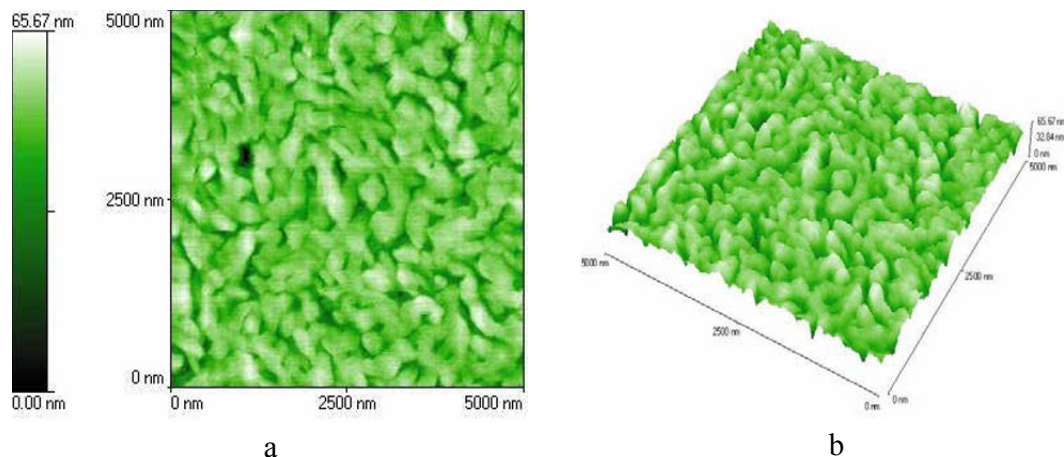


Fig. 4. $5\ \mu\text{m} \times 5\ \mu\text{m}$ AFM patterns of the surface of $\text{H}_2\text{Pc-Sp}$ thin films: (a) 2-D and (b) 3-D.

The molecular arrangement of the crystallites of phthalocyanine is clearly visible. The regular structure of phthalocyanine thin films is described as a stack of needle-like molecules with alternating tilt angles so that the molecules are arranged in zig-zag chains [12]. The phthalocyanine molecules are seen to be growing in parallel rows rather than in the zig-zag arrangement. The growth front of these crystallites forms an angle of about 55° to the rows of molecules. The precisely arranged rows of different crystals are tilted in the surface plane at about 25° to each other, and the space between

these rows are filled with molecules that are not well oriented [9].

Optical studies

The transmittance $T(\lambda)$ spectra of $\text{H}_2\text{PC-Th}$ and $\text{H}_2\text{PC-Sp}$ films are given in Fig. 5. The curves are similar in shape to each other, the discrepancy in $T(\lambda)$ intensities may be attributed to the thickness difference. There are two absorption bands in each curve. The Soret absorption band (B-band) is located at 356 nm. The strong absorption bands of at 670 and 739 nm, are due to the Q-band. Both arise from π to π^* transition [9, 13, 14].

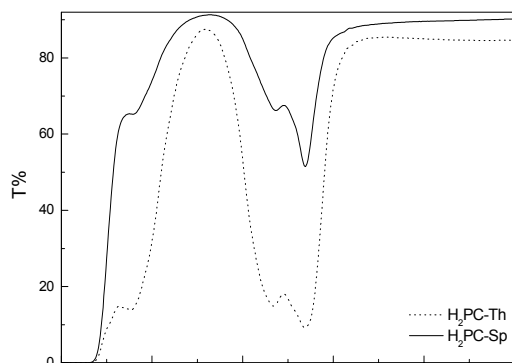


Fig. 5. The spectral behavior of transmittance $T(\lambda)$ of the $\text{H}_2\text{Pc-Th}$ and $\text{H}_2\text{Pc-Sp}$ thin films.

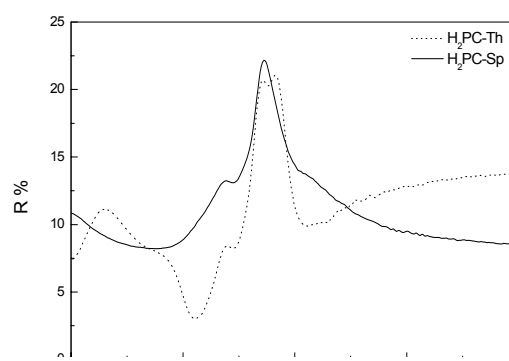


Fig. 6. The spectral distribution of reflectance $R(\lambda)$ of the $\text{H}_2\text{Pc-Th}$ and $\text{H}_2\text{Pc-Sp}$ thin films.

The spectral distribution of reflectance $R(\lambda)$ of the two thin films under investigation is shown in Fig. 6. As with Fig. 5, the two spectra here are also nearly identical. The main effect observed was that the film of H_2PC-Sp does not show the characteristic double intense peak that observed with the H_2PC-Th film in the range of 689–813 nm, this could be attributed to the difference in films thickness.

In Fig. 7, the absorption spectra, A , of the two films are shown as a function of photon energy. It can also be noticed that the two films are identical. As observed from this figure the Q-band shows the characteristic splitting (Davidov splitting) in all phthalocyanine derivatives which appears at 1.68 and 1.85 eV and has a value of 0.17 eV in agreement with other phthalocyanine compounds [15].

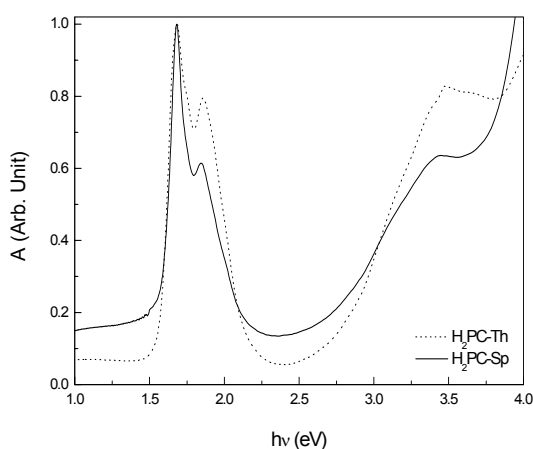


Fig. 7. The spectral distribution of absorbance $A(\nu)$ of the H_2PC-Th and H_2PC-Sp thin films.

It is quite clear from $T(\lambda)$ and $R(\lambda)$ results that at longer wavelengths ($\lambda > 900$ nm), all films become transparent and no light was scattered or absorbed as $T + R = 1$, i.e. non-absorbing region. The inequality $T + R < 1$ at shorter wavelengths

($\lambda < 900$ nm) implies the existence of absorption i.e. absorbing region.

The optical parameters refractive index, n , and the absorption index, k , for the thin films at different wavelength can be calculated by using the following equations [14]:

$$\alpha = \frac{1}{d} \ln \left[\frac{(1-R)^2}{2T} + \sqrt{\frac{(1-R)^4}{4T^2} + R} \right], \quad (2)$$

$$n = \left(\frac{1+R}{1-R} \right) + \sqrt{\frac{4R}{(1-R)^2} - k^2}, \quad (3)$$

$$k = \frac{\alpha \lambda}{4\pi}. \quad (4)$$

where α , d , and λ are the absorption coefficient, thin-film thickness, and wavelength of the incident light in air, respectively.

Using Eqs. (2) and (4) the variation of absorption coefficient, α , and the absorption index, k , with wavelength, λ in the range 300–1200 nm were calculated and are shown in Fig. 8 and 9. Neither α nor k were affected by the type of film deposition. Reduction in the peaks intensity of H_2PC-Th films might be due to the difference in film thickness.

The spectral distribution of refractive index $n(\lambda)$ for the two films under investigation was calculated from Eq. (3). The results are shown in Fig. 10 as a function of wave length, λ in the ranges 300–2700 nm and as a function of photon energy, $h\nu$ in Fig. 11. The different shape in $n(\lambda)$ of the two films may be ascribed to the thickness differences not to the method of preparation.

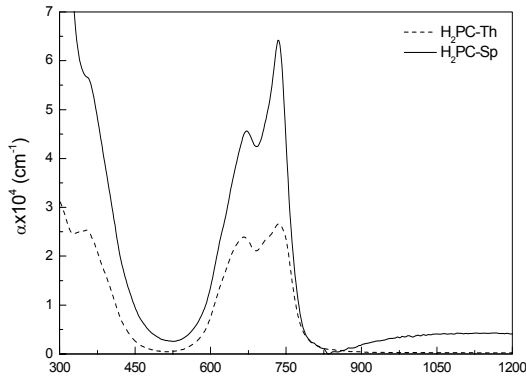


Fig. 8. The variation of absorption coefficient, α , as a function of wavelength, λ , for thermal and spin coated type of films.

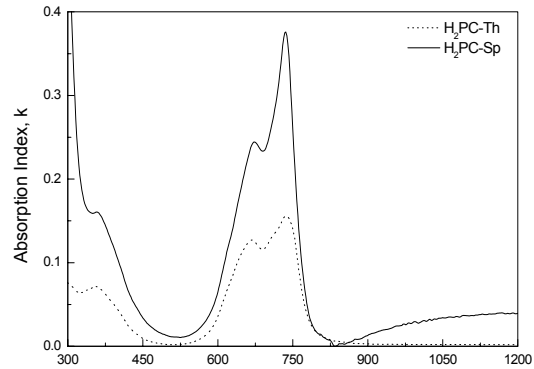


Fig. 9. The variation of the absorption index, k as a function of wavelength, λ for the H_2Pc -Th and H_2Pc -Sp thin films.

It is clear that dispersion curves (n, λ) can be divided into two regions. The curves exhibit anomalous dispersion in the wavelength range $\lambda < 820$ nm and normal dispersion for higher wavelengths. Fig. 9 shows normal dispersion in the range of wavelength 820–2700 nm. The refractive index of H_2Pc -Th increases slightly until about

1200 nm, then a very low rate of decrease is observable. On the other hand, the refractive index of H_2Pc -Sp decreases exponentially in the range of wavelength 820–2700 nm. Finally the refractive index becomes wavelength-independent above $\lambda \sim 2700$ nm for both thermal evaporated and spin coated films.

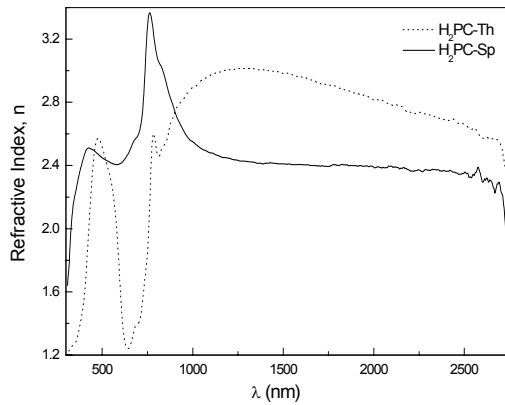


Fig. 10. The spectral distribution of refractive index $n(\lambda)$ for the H_2Pc -Th and H_2Pc -Sp thin films in the range 300–2700 nm.

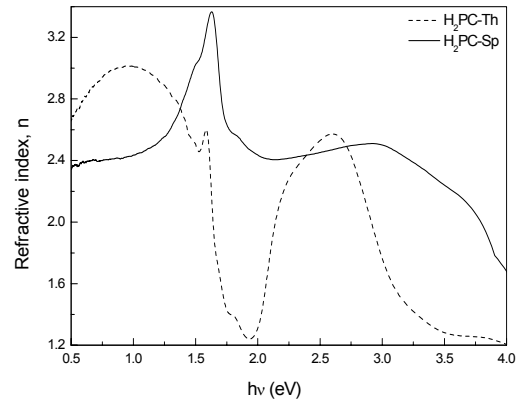


Fig. 11. The variation of the refractive index, n as a function of photon energy, $h\nu$ for the H_2Pc -Th and H_2Pc -Sp thin films.

To obtain information on direct and indirect inter-band transitions, the variation of absorption coefficient α with photon energy $h\nu$ and the

optical energy gap E_g are obtained from the following formula [13–17]:

$$\alpha = \alpha_0 (h\nu - E_g)^s, \quad (6)$$

where α_0 is a constant depends on the transition probability and the exponent S is an index which determines the types of transition and can take values of $1/2$, $3/2$, 2 , and 3 for allowed direct, forbidden direct, allowed indirect, and forbidden indirect transitions, respectively [16].

The optical absorption measurements for the phthalocyanine films indicate that the absorption mechanism is due to the indirect transition. The optical band gap of the indirect transition, E_g , can be obtained from the intercept of the $\alpha^{1/2}$ versus $h\nu$ plot with the energy axis.

A satisfactory fit was obtained for $\alpha^{1/2}$ as a function of $h\nu$, as shown in Fig. 12. The extrapolation of the straight line graphs $\alpha^{1/2} = 0$ gave the values of optical band gap E_g . The allowed indirect transition, E_g values were found almost equal and were determined as 2.96 and 2.94 eV for H_2Pc-Th and H_2Pc-Sp , respectively. The Q-band peaks also gave nearly an equal value as 2.33 and 2.5 eV for H_2Pc-Th and H_2Pc-Sp , respectively. The Q-band peaks also gave an equal value as 1.54 eV for H_2Pc-Th and H_2Pc-Sp , respectively.

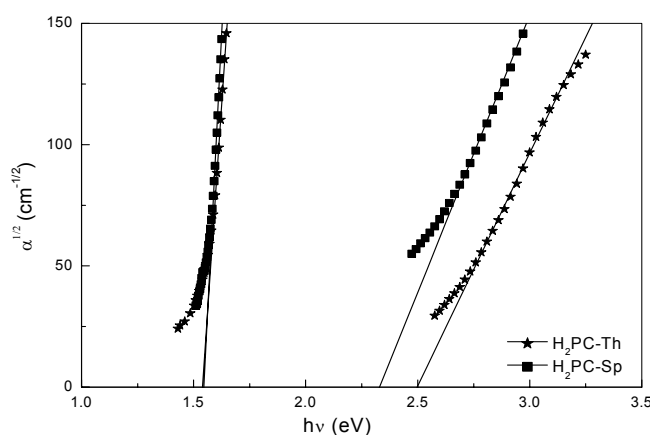


Fig. 12. Variation of $\alpha^{1/2}$ with photon energy $h\nu$ for the H_2Pc-Th and H_2Pc-Sp thin films.

Conclusion

The structure and optical properties of thermally evaporated, H_2Pc-Th and spin coated, H_2Pc-Sp metal-free 1, 4, 8, 11, 15, 18, 22, 25-octahexylphthalocyanine thin film of thickness 730 nm and 45-50 nm, respectively have been studied. The crystallite grain size was determined and found to be in the order of 88.65 and 44.32 nm for H_2Pc-Th and H_2Pc-Sp , respectively. Studies using AFM showed that the phthalocyanine molecules grow in parallel rows. The optical

properties of the thin films were studied in the range 300–1200 nm. The absorption spectra recorded show two absorption bands, the Soret band (B-band) at 356 nm and the Q-band with a doublet at 667 and 739 nm. The basic optical properties, namely optical absorption, coefficient, α , absorption index, n , and refractive index, k , were calculated. The optical measurements indicate that the absorption mechanism is due to both the indirect transition.

References

- [1] Leznoff, C. C., Lever, A.B.P. (1989). Phthalocyanine-Properties and Applications, Vol. **1**, VCH, New York.
- [2] Leznoff, C.C., Lever, A.B.P. (1993) Phthalocyanine-Properties and Applications, Vol. **3**, VCH, New York,.
- [3] Evans, D. A., Steiner, H.J., Middleton, R. Jones, T.S., Chen, C.H., Horn, K., Park, S., Kampen, T. U., Tenne, D., Zahn, D. R. T., Patchett, A., McGovern, I.T. (2001). Appl. Surf. Sci. **175,176**: 374
- [4] Rella, R., Serra, A., Siciliano, P., Tepore, A., Valli, L., Zocco, A. (1997). Supramol. Sci. **4**: 461.
- [5] Cook, M.J. (1996). J. Mater. Chem. **6**: 677.
- [6] Hassan, B. M., Li, H., McKeown, N. B. (2000). J. Mater. Chem. **10**: 39.
- [7] Ali-Adib, Z., Clarkson, G. J., McKeown, N. B., Treacher, K.E., Gleeson, H. F., Stennett, A. S. (1998). J. Mater. Chem. **8**: 2371.
- [8] Al-Raqa, S. Y., Solieman, A. S., Joraid, A. A., Alamri, S. N., Moussa, Z., Aljuhani, A. (2008) Polyhedron **27**: 1256.
- [9] Alamri, S. N., Joraid, Al-Raqa, S. Y. (2006). Thin Solid Films **510**: 265.
- [10] Al-Raqa, S. Y. (2008). Dyes Pigments **77**: 259.
- [11] Narayanan Unni, K. N., Menon, C. S. (2000). Mater. Lett. **45**: 326.
- [12] Cook, M. J., Chambrier, I. (2003) In: K.M. Kadish, K. M. Smith, R. Guillard (Eds.), Phthalocyanine Thin Films: Deposition and Structural Studies, The Porphyrin Handbook, vol. **17**, Academic Press,.
- [13] Narayanan Unni, K. N. (2003). Mater. Lett. **57**: 2215.
- [14] El-Nahass, M. M., Atta, A. A., El-Sayed, H. E. A., El-Zaidia, E. F. M. (2008). Applied Surface Science **254**: 2458.
- [15] El-Nahass, M. M., Farag, A. M., Abd El-Rahman, K. F., Darwish, A. A. A. (2005). Optics & Laser Technology **37**: 513.
- [16] El-Nahass, M. M., Abd-El-Rahman, K. F., Ghamdi, A. A., Asiri, A. M. (2004). Physica B, **344**: 398.
- [17] El-Nahass, M. M., Sallam, M. M., Ali, H. A. (2005). Inter. J. Mod. Phys. B, **19**: 4057.